Journal of Electrical Engineering, Electronics, Control and Computer Science – JEEECCS, Volume 7, Issue 26, pages 41-52, 2021

Harmonic pollution control of electrical networks: Comparative study of controls, by Pulse Width Modulation, Duty Cycle Modulation and Symmetrical Linear Duty Cycle Modulation of the three-phase shunt active Parallel filters

Fabrice Biloa Assolo[1], Charles Hubert Kom[1, 2], Arnaud Nanfak[2], Gildas Martial Ngaleu[2]
[1] Research Laboratory of Computer Science Engineering and Automation
Higher Normal School of Technical Education,
University of Douala, Po Box 2701 Douala, Cameroon
[2]Laboratory of Energy, Materials, Modelling and Methods,
Higher National Polytechnic School of Douala
University of Douala, Po Box 2701 Douala, Cameroon
[1]fabricebiloa@yahoo.fr, [2]charleshubert.kom@gmail.com, [2]nanfak.arnaud@yahoo.fr, [2]gmngaleu@yahoo.fr

Abstract **– The increasing use on electrical networks of consumer electronic devices (televisions, computers) and industrial electronic devices (variable speed drives, high efficiency lighting) pollutes these networks by harmonic currents and voltages. The three-phase active shunt filter is a modern solution for the remediation of three-phase electrical networks. Better pollution control requires proper sizing of the active shunt filter. Indeed, the capacity and adaptability of the filter reside in the quality of the control of the switches of the inverter constituting it. In this article we are interested in controlling inverters. A comparative study of Pulse Width Modulator (PWM) controls, Duty Cycle Modulation inverter (DCM) control and Symmetrical Linear Duty Cycle Modulation (SLDCM) control in a three-phase network. The study shows that the DCM inverter gives the best results with regard to the reduction of harmonic pollution, and therefore of the quality of the network.**

Keywords: shunt active parallel filter, Harmonic pollution, PWM control, DCM control, SLDCM control

I. INTRODUCTION

The development of power electronics and the increase in the powers involved as well as the flexible use of semiconductors, an encouraged electrical engineer to undertake important associations of static converters power to electrical machines. These devices are usually loads that are not linear, which absorb a non-sinusoidal current and behave like harmonic generators. Of moreover, they sometimes consume reactive energy. Therefore, the waveform of the current of the source loses its sinusoidal shape and we obtain also a degradation of the power factor. Through therefore, distributors of electrical energy see themselves therefore obliged to impose standards and protect themselves against these disturbances. One of the solutions used is passive filtering: it consists in trapping the currents harmonics in LC circuits, tuned to the ranks of harmonics to be filtered. Rows 5 and 7 are the most commonly filtered. However, this solution is moderately effective [1] - [2]. Common use of devices power electronics, made it possible to design self-adapting harmonic elimination devices called active compensators harmonics, or active filters. These filters the main objective of the assets is to compensate for harmonic currents injected into the network [3] [4] [5].

Our work then turned to the study of the control-command block of the active filter. There are several types of control of three-phase shunt filters for this purpose which have been presented in the literature. There are several techniques to control the compensating current injection such as a Pulse Width Modulation (PWM) Duty Cycle Modulation (DCM) and new duty-cycle modulator structures namely Symmetrical Linear DCM (SLDCM). PWM technique is a modulation technique in which the frequency can be either constant or variable[6]. In constant frequency PWM method, the frequency is constant and the ON time changes according to the modulating signal. It can be produced by comparing a reference signal with a carrier signal[6]. In variable frequency PWM method, the frequency is variable and ON time or OFF time is constant. In variable frequency PWM method, the frequency is variable and ON time or OFF time is constant. There are several different PWM techniques, differing in their methods of implementation. The basics PWM topologies including single PWM produced by comparing rectangular reference wave with triangular carrier wave, the multiple PWM and the Sinusoidal PWM (SPWM) using sinusoidal reference wave and triangular carrier wave [7].

The duty cycle modulation (DCM) is a modulation in which an input signal x is transformed into a train of switching wave where duty cycle and period of the modulated signal vary simultaneously according to control signal [8] [7]. The DCM technique has been used in several application areas.

From instrumentation to process control, including Signal processing. Thus, a scientific article on the application of the principle of modulation of duty cycle in instrumentation has been published [9]. In this article, a class of new DCM is investigated. It used the analog signal processing techniques with a simple operational amplifier circuit. The first papers to use DCM as an analog-to-digital converter are[10] [11]. These two papers respectively presented the feasibility of analog-to-digital conversion by DCM via virtual simulations and the multi-channel version of A/D conversion based on the use of duty cycle modulator cells in parallel, each used as a circuit.

In [12], buck converters use the DCM control technique. In this article, analytical developments, numerical analysis, virtual simulations and experimentation have demonstrated that DCM control system provides better characteristics compared to standard PWM techniques, so DCM control can be considered as a new perspective of control in power electronics and control engineering [13], with a possible extension to other CC-CC converters [14], even to the important class of DC-AC inverters [15].

The article[16] makes the comparative study of IGBT controls between DCM and hysteresis in a three-phase network, it emerges that the DCM control offers the best performance in terms of harmonic rate reduction.

The new DCM modulator structures are proposed in [17]. These are Symmetric Linear DCM (SLDCM) and General Linear DCM (GLDCM). These two structures consist of integrator circuits, a hysteresis comparator and advantages of PWM and DCM circuits.

In this paper, our objective is to make a comparative study followed by simulation in the software MATLAB / SIMULINK, of the controls by PWM, DCM of the inverter and SLDCM of an SAPF (Shunt Active parallel Filter) for harmonic pollution control application.

The article is organized as follows. In section II, we present the methodology used. In section III, we present the simulation results. And we end with a conclusion where we highlight the value of this best-performing ordering strategy.

II. METHOD

A. Principle of parallel active filter

This filter is connected in parallel on the network. The principle of the parallel active filter consists in generating currents in opposition of phase to the harmonic currents existing on the network and created by the nonlinear loads. In this way, the current supplied by the energy source remains sinusoidal. The parallel active filter consists of two blocks: the power part and the control-command part Figure.1.

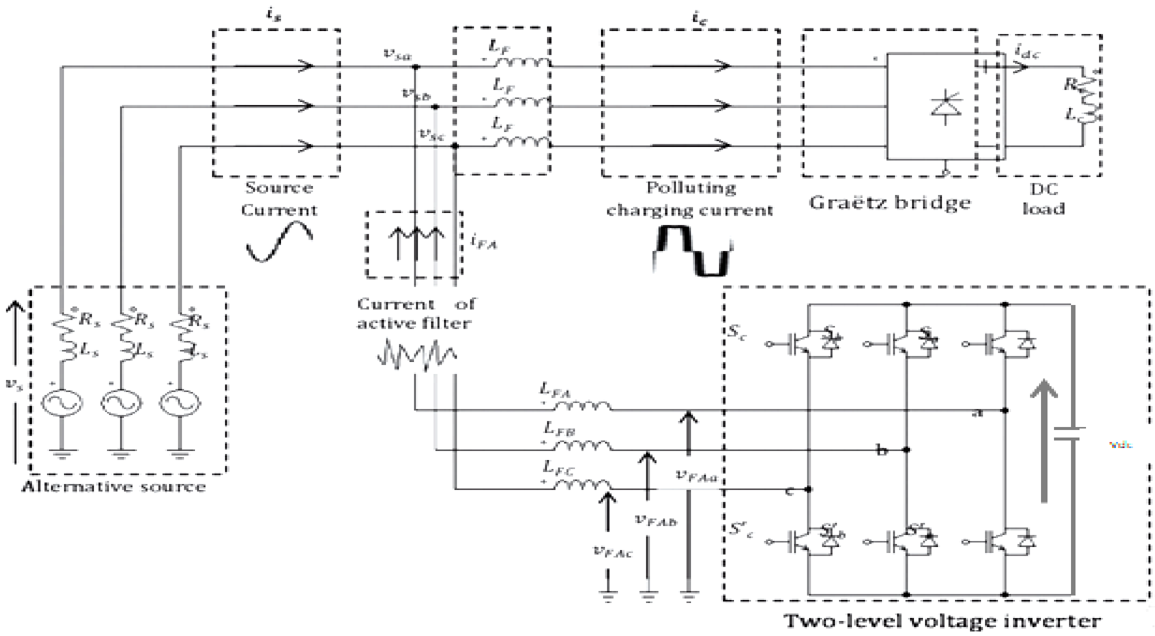

Figure 1: Principle of the parallel active filter [18]

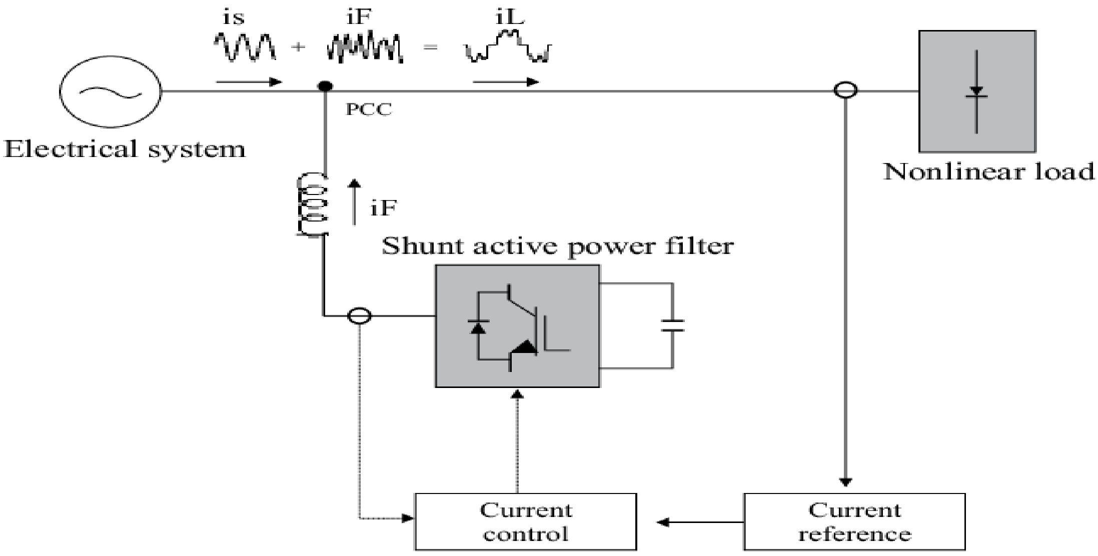

Figure 2: Main blocks in the electrical circuit for a shunt active power filter

Concerning Figure 2, we can identify the main block of our study: the current control because it is in this block that we will apply in turn the command PWM, DCM inverter and SLDCM to switch the IGBTs of the inverter. In the second current reference block, we will apply the instantaneous powers algorithm to identify the reference currents.

B. Theory of instantaneous powers

The instantaneous active and reactive power method was developed by Akagi [19] and uses the Concordia transformation of phase-to-neutral voltages Vs and line currents Is, in order to calculate instantaneous active and reactive powers. The principle of this classical method is now briefly described. Let respectively be the phase-to-neutral voltages of a three-phase network without zero sequence (connected to a polluting load) and the three load currents, denoted v_{sa}, v_{sb}, v_{sc} and i_{c1}, i_{c2}, i_{c3}. The Concordia transformation makes it possible to reduce this balanced three-phase system to a two-phase system whose axes are in quadrature:

$$\begin{bmatrix} V_{s\alpha} \\ V_{s\beta} \end{bmatrix} = \sqrt{\frac{2}{3}} \begin{bmatrix} 1 & -\frac{1}{2} & -\frac{1}{2} \\ 0 & \frac{\sqrt{3}}{2} & -\frac{\sqrt{3}}{2} \end{bmatrix} \begin{bmatrix} V_{sa} \\ V_{sb} \\ V_{sc} \end{bmatrix} \quad (1)$$

$$\begin{bmatrix} I_{s\alpha} \\ I_{s\beta} \end{bmatrix} = \sqrt{\frac{2}{3}} \begin{bmatrix} 1 & -\frac{1}{2} & -\frac{1}{2} \\ 0 & \frac{\sqrt{3}}{2} & -\frac{\sqrt{3}}{2} \end{bmatrix} \begin{bmatrix} I_{ca} \\ I_{cb} \\ I_{cc} \end{bmatrix} \quad (2)$$

Instantaneous active power p and instantaneous reactive power q are defined by:

$$\begin{bmatrix} \boldsymbol{p} \\ \boldsymbol{q} \end{bmatrix} = \begin{bmatrix} v_\alpha & v_\beta \\ -v_\beta & v_\alpha \end{bmatrix} \begin{bmatrix} i_\alpha \\ i_\beta \end{bmatrix} \quad (3)$$

Instantaneous active and reactive powers can be written as the sum of a DC component and an AC component:

$$\begin{bmatrix} \boldsymbol{p} \\ \boldsymbol{q} \end{bmatrix} = \begin{bmatrix} \overline{p} + p \\ \overline{q} + q \end{bmatrix} \quad (4)$$

From equation (4), we can deduce the expressions for the components of the charging current along the αβ axes:

$$\begin{bmatrix} i_\alpha \\ i_\beta \end{bmatrix} = \begin{bmatrix} V_\alpha & V_\beta \\ -V_\beta & V_\alpha \end{bmatrix}^{-1} \begin{bmatrix} p \\ -q \end{bmatrix}$$
$$\Rightarrow \begin{bmatrix} i_\alpha \\ i_\beta \end{bmatrix} = \frac{1}{V_\alpha^2 + V_\beta^2} \begin{bmatrix} V_\alpha & -V_\beta \\ V_\beta & V_\alpha \end{bmatrix} \begin{bmatrix} p \\ -q \end{bmatrix} \quad (5)$$

By replacing (4) in (5), these currents are expressed along the αβ axes by:

$$\begin{bmatrix} i_\alpha \\ i_\beta \end{bmatrix} = \frac{1}{V_\alpha^2 + V_\beta^2} \begin{bmatrix} V_\alpha & -V_\beta \\ V_\beta & V_\alpha \end{bmatrix} \begin{bmatrix} \overline{p} \\ -\overline{q} \end{bmatrix} + \frac{1}{V_\alpha^2 + V_\beta^2} \begin{bmatrix} V_\alpha & -V_\beta \\ V_\beta & V_\alpha \end{bmatrix} \begin{bmatrix} p \\ -q \end{bmatrix} \quad (6)$$

Finally, it is easy to obtain the reference currents along the abc axes by the inverse transformation of Concordia:

$$\begin{bmatrix} i_{ref1} \\ \boldsymbol{i_{ref2}} \\ \boldsymbol{i_{ref3}} \end{bmatrix} = \sqrt{\frac{2}{3}} \begin{bmatrix} 1 & 0 \\ -\frac{1}{2} & \frac{\sqrt{3}}{2} \\ -\frac{1}{2} & -\frac{\sqrt{3}}{2} \end{bmatrix} \begin{bmatrix} i_{ref\alpha} \\ i_{ref\beta} \end{bmatrix} \quad (7)$$

Figure 3 gives the implementation algorithm of the instantaneous power method to obtain the reference currents. The two-phase current method works in the space of αβ currents. It therefore requires fewer calculations while being more precise and more robust than other methods.

a change of reference point of the load currents and the network voltages is carried out using Concordia to switch from three-phase to two-phase (αβ). Afterwards the reactive and active powers are calculated. At this stage, to obtain the AC components, two low-pass filters are used respectively for the active and reactive power. The calculation of the reference currents in the αβ benchmark is carried out thanks to the alternating components of the powers of the voltage and of the regulated voltage of the inverter. Finally to obtain the final result we apply the inverse transform of Concordia

:

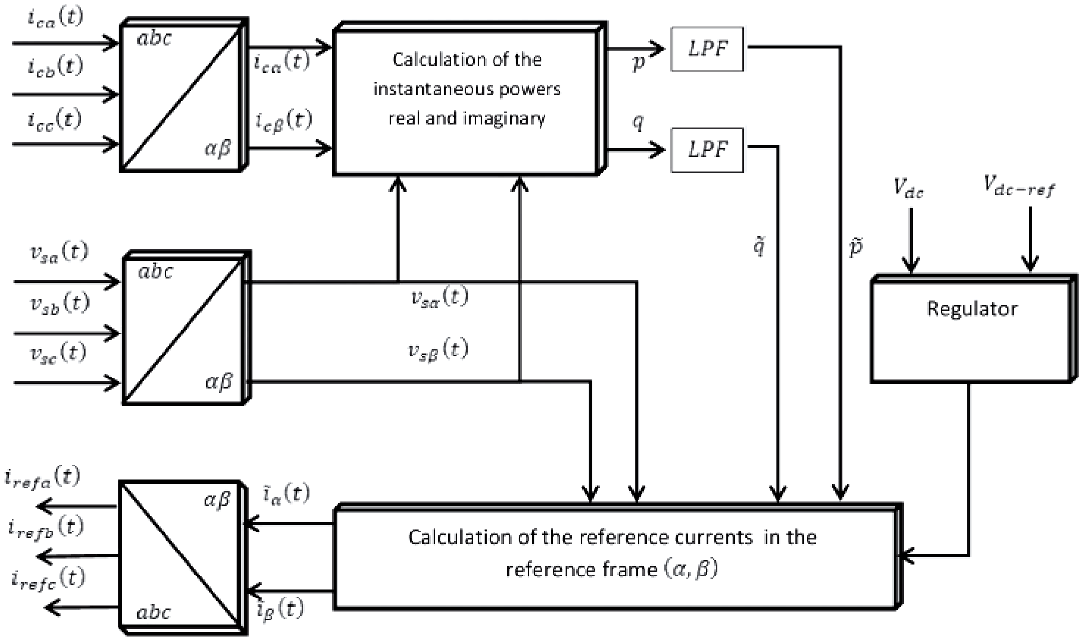

Figure 3: Generation of reference currents by the instantaneous power method

C. Control by PWM of the active filter invert

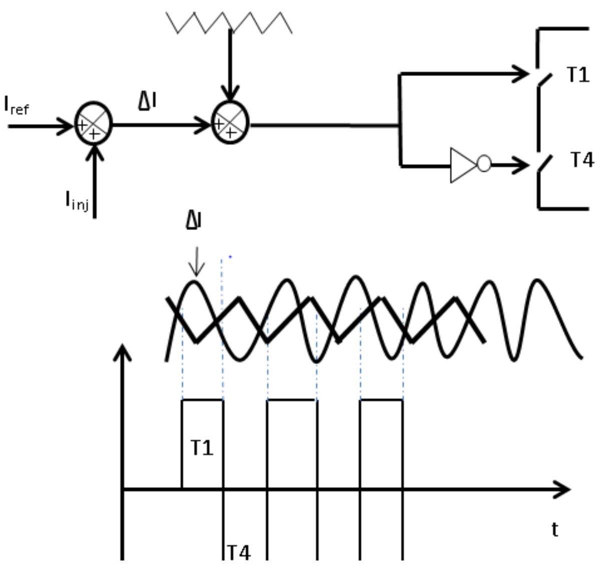

Figure 4: PWM control principle

In [20] the different PWM techniques are presented: the PWM with symmetric regular sampling, the PWM with asymmetric regular sampling and the PWM with natural sampling. The technical diagram of the PWM is given in Figure 4 each group of transistor-diode assembled in parallel forms a bi-controllable switch. The previous technical diagram first uses a regulator which determines the reference voltage of the inverter (modulator) from the difference between the measured current and its reference. The latter is then compared with a triangular signal called a high frequency carrier in this work it is a 200 Hz setting the switching frequency. The output of the comparator provides the command order of the switches.Figure 5 gives the Simulink model of the PWM control where the reference currents come from the instantaneous power unit PQ.

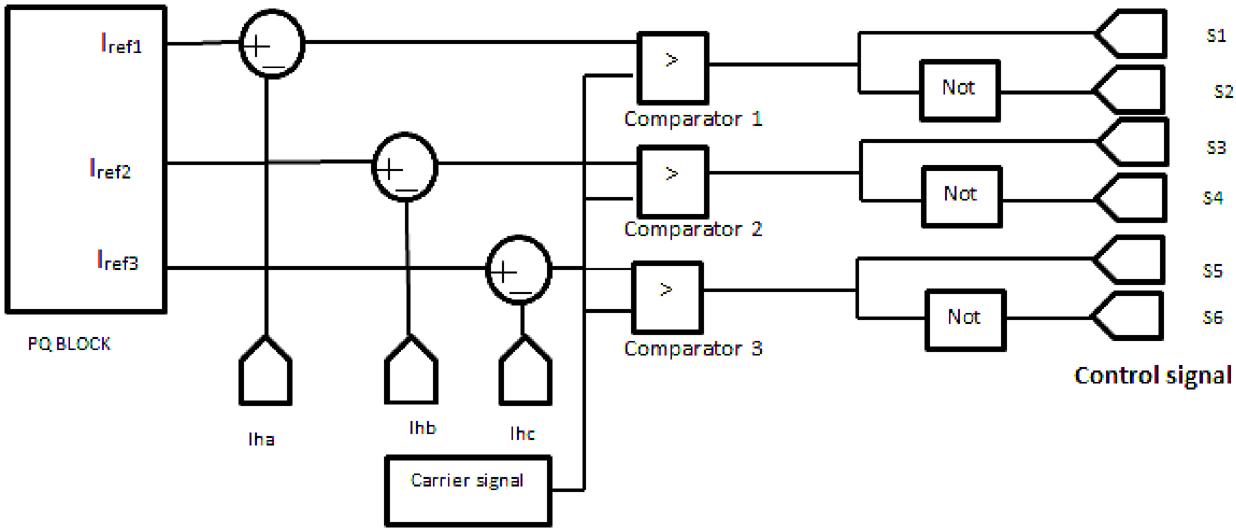

Figure 5: Command by PWM in MATLAB/SIMULINK

D. Control by DCM of the inverter of the active three-phase shunt filter

The duty cycle modulation technique (DCM) translates new perspectives in inverter control techniques. DCM consists in transforming a signal Vref (reference intensity) into a modulated signal Vs (t).± Vcc, produces an all-or-nothing modulated signal, thus protecting the transmitted signal from noise. Non-inverting DCM is used in this case because it varies according to the modulation signal. Its operating principle is described in figure 6

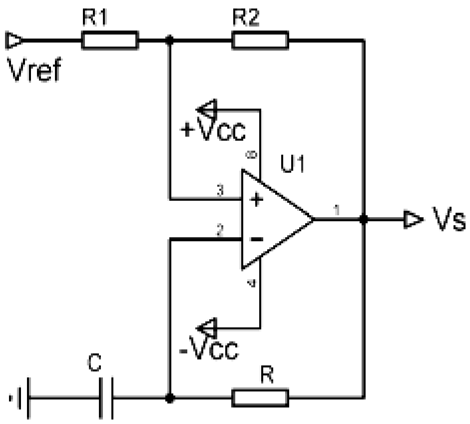

Figure 6: Non-inverter duty-cycle modulator [17]

The principle of duty cycle modulation (DCM) is based on encoding in the duty cycle Rm=Ton (t)/Tm (t) of a square wave signal of the reference analog signal Vref (t). A DCM circuit therefore behaves like a voltage controlled oscillator. It consists therefore in a modulator involving a high relaxation frequency of the oscillator and a low frequency of the control signal to be modulated. Thus, the resulting modulated voltage Vs (t) is related to the associated switching control signal, the switching being ensured by an operational amplifier in its non-linear operation. The saturation voltages of the amplifiers are +Vsat and -Vsat while +VCC and -VCC are their supply voltages The mathematical model DCM in our shunt filter is

$$V_s(t) = \begin{cases} V_{sat} \ \ if\ u^+ > u^- \\ -V_{sat}\ if\ u^+ < u^- \end{cases}$$
$$\Rightarrow u^+ = \begin{cases} \alpha V_{sat} + \alpha_1 V_{ref} \ \ if\ \ V_s(t) = V_{sat} \\ -\alpha V_{sat} + \alpha_1 V_{ref}\ if\ V_s(t) = -V_{sat} \end{cases} \quad (8)$$

With

$$\alpha = \frac{R_1}{R_1 + R_2}$$
$$\alpha_1 = \frac{R_2}{R_1 + R_2} \quad (9)$$

The supply voltage of the capacitor is governed by a differential equation:

$$RC\frac{du_c(t)}{dt} + u_c(t) = V_s(t) \quad (10)$$

A solution of this equation is:

$$u_c(t) = (u_i - u_f)e^{-t/RC} + u_f \quad (11)$$

The capacitor charge and discharge times are included respectively 0 <t <T1 and T1 <t <T2 It is established that:

$$T_1 = -\tau ln\left(\frac{\alpha_1 V_{ref} + (\alpha - 1)V_{sat}}{\alpha_1 V_{ref} - (1-\alpha)V_{sat}}\right) \quad (12)$$

$$T_2 = -\tau ln\left(\frac{\alpha_1 V_{ref} - (\alpha - 1)V_{sat}}{\alpha_1 V_{ref} + (1+\alpha)V_{sat}}\right) \quad (13)$$

$$T = \tau ln\frac{\alpha_1 V_{ref} - (\alpha-1)V_{sat}}{\alpha_1 V_{ref} + (1+\alpha)V_{sat}} + \tau ln\frac{\alpha_1 V_{ref} + (\alpha-1)V_{sat}}{\alpha_1 V_{ref} - (1-\alpha)V_{sat}}$$

$$\Rightarrow T = RC\ln\left(\frac{(\alpha_1 V_{ref})^2 - ((\alpha-1)V_{sat})^2}{(\alpha_1 V_{ref})^2 - ((1-\alpha)V_{sat})^2}\right) \quad (14)$$

$$\tau = RC$$

The duty cycle of the non-inverting modulator is:

$$R_m = \frac{T_1(V_{ref})}{T_m(V_{ref})} \quad (15)$$

we deduct:

$$R_m(V_{ref},\alpha,V_{sat}) = \frac{\ln(\frac{\alpha_1 V_{ref} - (\alpha-1)V_{sat}}{\alpha_1 V_{ref} + (1+\alpha)V_{sat}})}{\ln(\frac{(\alpha_1 V_{ref})^2 - ((\alpha+1)V_{sat})^2}{(\alpha_1 V_{ref})^2 - ((1-\alpha)V_{sat})^2})} \quad (16)$$

In order to improve the efficiency of the electronic parts of the non-inverting DCM modulator, we are optimizing our modulator. The aim is to find the optimal characteristic parameters α, τ and E of the modulator providing an excellent level of operation. For this purpose, the effects of non-linearity and variation of the characteristic parameters were studied. The optimal quality of the modulator obtained is observed through its characteristic quantities: $R_m(V_{ref},\alpha,V_{sat})$ and $f_m = \frac{1}{T(V_{ref},\alpha,V_{sat},\tau)}$ with f_m being the frequency of the modulator and $R_m(V_{ref},\alpha,V_{sat})$ the duty cycle.

Optimizing the MRC modulator therefore means maximizing $Pm(\alpha,V_{sat})$ or minimizing $-P_m(\alpha,V_{sat})$ Which is the slope. Our optimization criterion is therefore $Pm(\alpha,V_{sat})$ or

$$P_m = \frac{\alpha}{V_{sat}(1+\alpha)\log(\frac{1+\alpha}{1-\alpha})} \quad (17)$$

$$\begin{cases} f_{m0} = \dfrac{1}{2\tau\ln(\frac{1+\alpha}{1-\alpha})} \\ f_{\min} = \dfrac{1}{\tau\ln\left[\frac{(\alpha_1 V_{\max})^2 - ((1+\alpha)V_{sat})^2}{(\alpha_1 V_{\max})^2 - ((\alpha-1)V_{sat})^2}\right]} \\ 0 \prec \alpha \prec 1 \end{cases} \quad (18)$$

With the basic frequency of the modulator f_{m0} previously selected, the minimum frequency f_m previously established α=0.003081723734398

τ =RC with f_{mlim} is the limit modulator frequency. Our work on optimization is based on the formulation given in [16] and for the chosen f_{m0} equal to 200 KHz, the frequency f_{mlim} is obtained by calculating f_{min} for α very small. We obtain the following optimum parameters of DCM:

α=0.003081723734398 or

$\alpha=R_1/(R_1+R_2)$ and $1-\alpha=R_2/(R_1+R_2)$

After calculating the value τ=0.000486670905896s, R1=330Ω, R2=10KΩ, C=47nF, R=1KΩ

Figure.7 represents the Simulink diagram of the DCM modulator. The latter's input is Iref and its output is cmd. Its parameters were determined in the previous paragraph.

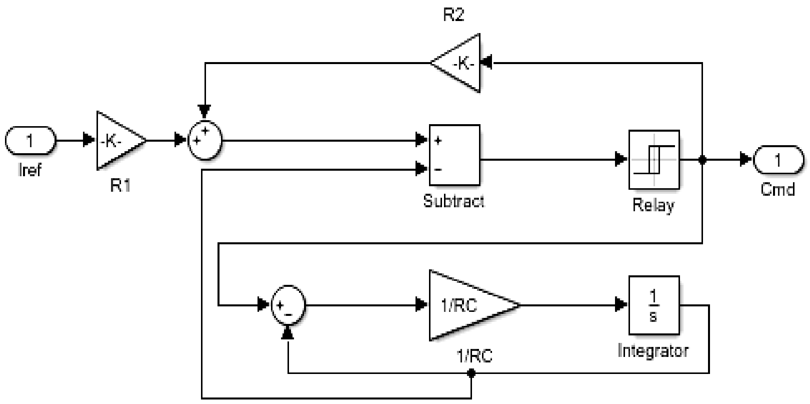

Figure 7: Command by DCM in MATLAB/SIMULIN

E. Symmetrical Linear Duty-Cycle Modulation

Figure. 8 gives the operating principle of the SLDCM. The hysteresis comparator obtained the signal and the integrator modulates by integrating the difference between the modulated signal and the reference signal, a triangular signal is a return to the input of the comparator.

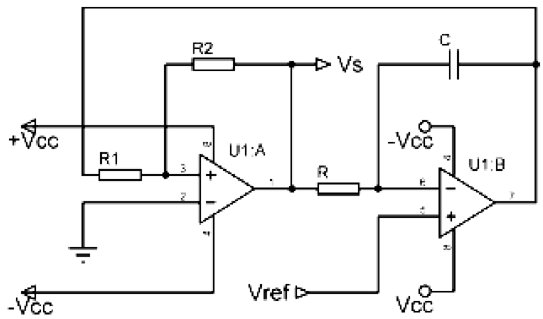

Figure 8: Symmetrical Linear Duty-Cycle Modulation [17]

The mesh law applied to the voltages on the first non-inverting modulator gives the equations below:

$$v_o R_2 + V_s R_1 = 0 \tag{19}$$

$$v_o = -\frac{R_1}{R_2} V_s \tag{20}$$

vo represents both the integrator output voltage and the input to the control signal switching block. The current in the capacitor C is defined by:

$$\begin{cases} v_0^+ = +\dfrac{R_1}{R_2} V_{sat} \\ v_0^- = -\dfrac{R_1}{R_2} V_{sat} \end{cases} \tag{21}$$

The current in the capacitor **C** is defined by:

$$i_c = \frac{V_s - V_{ref}}{R} = C\frac{dv_c}{dt} \tag{22}$$

Where, v_c is the voltage across the capacitor.
The output voltage v_0 of the integrator is given by:

$$\begin{aligned} & v_0 = V_{ref} - v_c \\ & \Leftrightarrow v_c = V_{ref} - v_0 \end{aligned} \tag{23}$$

So,

$$dt = \frac{RC}{V_s - V_{ref}} (dV_{ref} - dv_0) \tag{24}$$

If $dV_{ref} = 0$ then Vref is a constant so

$$dt = -\frac{RC}{V_s - V_{ref}} dv_0 \tag{25}$$

Now let's calculate t_{on} and t_{off}

During t_{on}, $V_S=+V_{sat}$ and v_0 goes from v_0^+ to v_0^-

$$t_{on} = -\frac{RC}{V_{sat} - V_{ef}} \int_{v_0^+}^{v_0^-} dv_0 \tag{26}$$

$$t_{on} = 2RC\frac{R_1}{R_2}\frac{V_{sat}}{V_{sat} - V_{ref}} \tag{27}$$

During t_{on}, $V_S=-V_{sat}$ and v_0 goes from v_0^- to v_0^+

$$t_{0FF} = 2RC\frac{R_1}{R_2}\frac{V_{sat}}{V_{sat} + V_{ref}} \tag{28}$$

So, T= $t_{on} + t_{OFF}$ (29)

$$T = 4RC\frac{R_1}{R_2}\frac{V_{sat}^2}{V_{sat}^2 - V_{ref}^2} \tag{30}$$

α Which represents the duty cycle is equal to:

$$\alpha = \frac{t_{on}}{T} = \frac{1}{2}\left(1 + \frac{V_{ref}}{V_{sat}}\right) \tag{31}$$

The duty cycle of SLDCM is a linear equation (30) consisting only of the passive components. When Vref = 0v the respective values of its minimum periods and are duty cycles are equal to:

$$\begin{cases} T_0 = 4RC\dfrac{R_1}{R_2} \\ \alpha = \dfrac{1}{2} \end{cases} \tag{32}$$

III. SIMULATION AND RESULTS

A. Simulation parameter

Simulations in MATLAB/SIMULINK were carried out under the specifications found in Table 1 below.

The parameters of the simulations are grouped together in table 1. Regarding the DCM parameters, we use the data from[16] whose optimization parameters were determined in section II with a frequency of 200 hz. on the other hand the parameters of the SLDCM use the data of [17]which were provided experimentally in this article. The frequency value of SLDCM is 200HZ. Finally, the frequency of the PWM carrier is 200Hz compared to a frequency of 50Hz to produce the IGBT control slots.

The simulated electrical network is three-phase three-wire and the MATLAB/Simulink software is used. The pollutant load is a conventional three-phase rectifier connected in series in an electrical network

TABLE 1: SIMULATION PARAMETERS

Source	Vs=220V,f=50Hz, Rs= $0.25\text{x}10^{-3}\Omega$
Load	Lc=0.023 mH, Rc=0,82mΩ, =0,78mΩ, Lc=2,6mH
Filter	L_f=3mH, C=8mF
DCM	R1=330Ω, R2=10KΩ, C=47nF, R=1KΩ
SLDCM	R1=10KΩ, R2=20KΩ, C=10nF, R=5.000KΩ

.

The general structure of the studied system is given in Figure. 9, the system is constituted:

- A three-phase power source,
- A non-linear charge,
- An active three-phase shunt filter connected in parallel to the mains,
- A filter control unit.

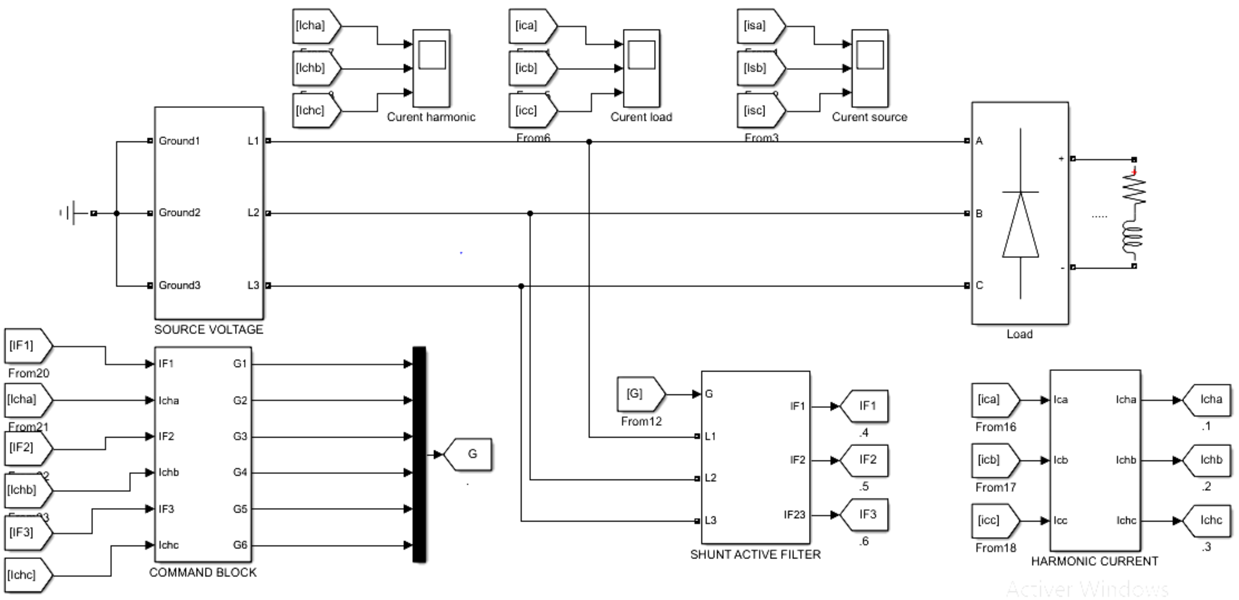

Figure 9: The general structure of the system studied

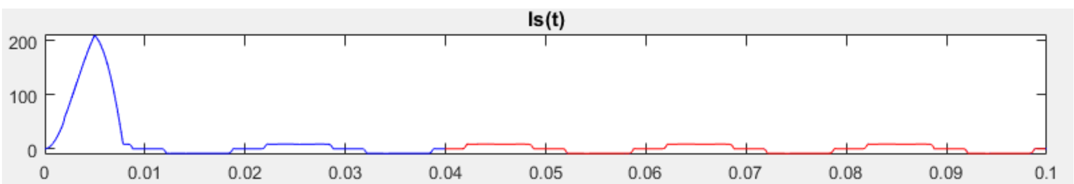

Figure 10: Waveform of the load and source Is(t) before filter

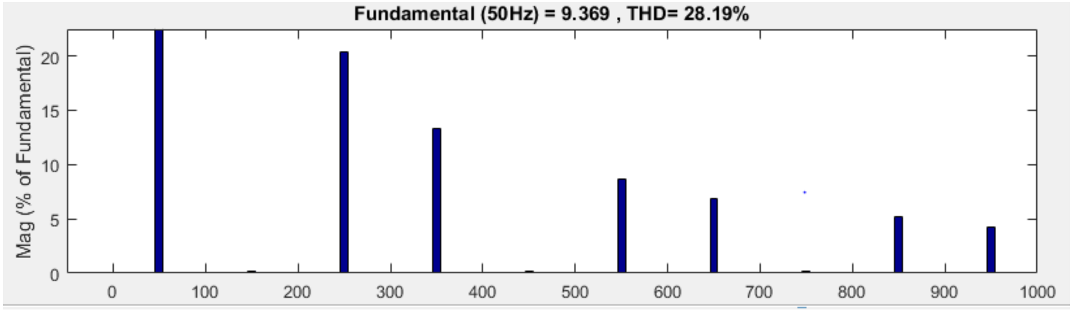

Figure 11: Order of source current harmonics and TDH before shunt active filter

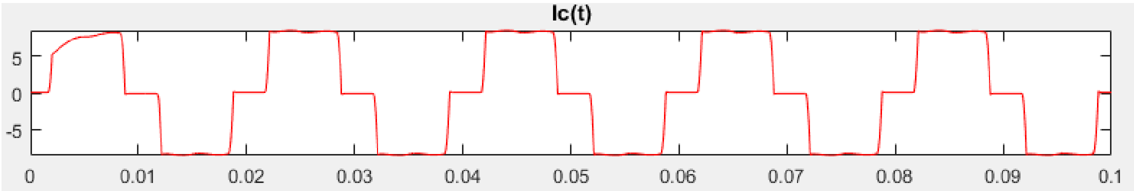

Figure 12: Waveform of the load

Figure. 10 shows the course of the current Is(t) in the network before filtering for phase (a), the spectral analysis of this current is presented in Figure. 11 source harmonics spectrum contains the harmonics of rank 5,7,13,17 and 19. And we observe the presence of several ranks of harmonics disturbing the current waveform, i.e. a THD of 28.197%. Figure. 12 is a waveform of the load current main actors of said deformations because it does not consume the sinusoidal energy produced by the source it then injects into the circuit of harmonics.

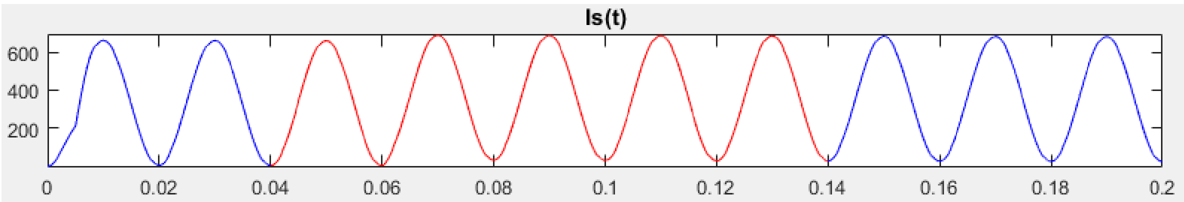

Figure 13: Waveform of the current source Is(t) after filter: control by PWM

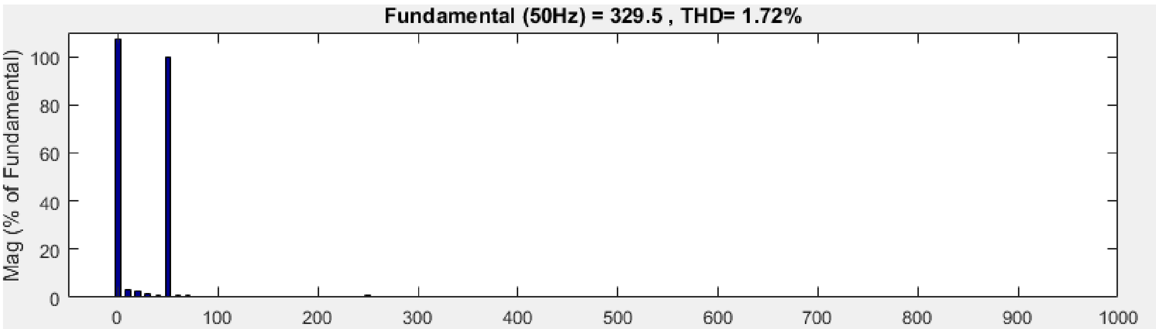

Figure 14: Order of source current harmonics and TDH after shunt active filter: control by PWM

Figure. 13 and 14 are the characteristics obtained from the source current after filtering using the PWM control, thus obtaining respectively the waveform which has become sinusoidal again, proof that there has been a reduction in harmonics and the harmonic rate which has passed from 28.19% THD to 1.72%, the result of which complies with the IEEE-519 standard which must meet the condition that the THD must be less than 5%.

After filtering the current Is(t) by the active shunt filter controlled by PWM control, we obtain the signal in Figure. 13. We observe a significant improvement in the waveform which has become sinusoidal and whose spectrum given in Figure 14 allowing us to affirm that there is a clear decrease in harmonics, i.e. a THD of 1.72%.

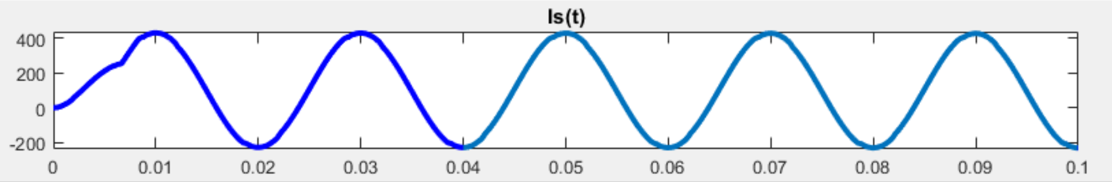

Figure 15: Waveform of the current source Is(t) after filter: control by DCM

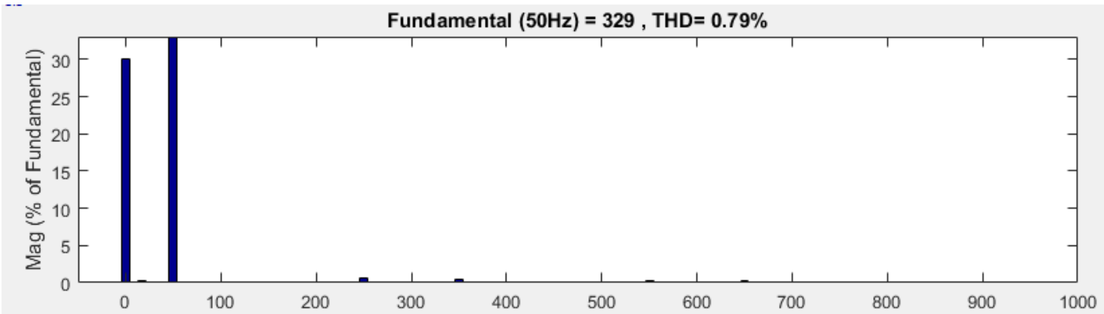

Figure 16: Order of source current harmonics and TDH after shunt active filter: control by DCM

By applying the control by Modulation with DCM to our active shunt filter we obtain the signal Is(t) in Figure 15 which shows a significant improvement in the curve and whose current spectrum Is(t) in Figure 16 shows a greater reduction in harmonics, i.e. THD = 0.79%.

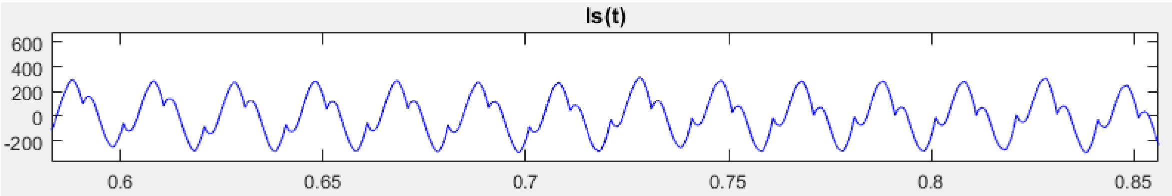

Figure 17: Waveform of the current source Is(t) after filter: control by SLDCM

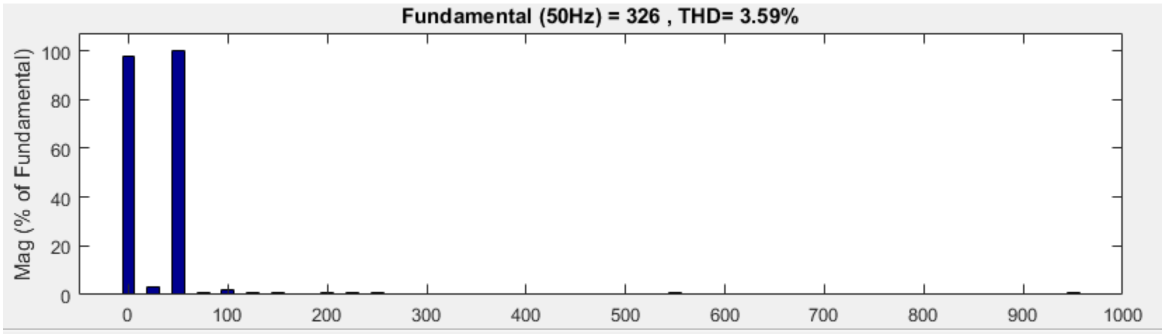

Figure 18: Order of source current harmonics and TDH after shunt active filter: control by SLDCM

By applying the control by Modulation with SLDCM to our active shunt filter we obtain the signal Is(t) in Figure 17 which shows a slight degradation at the level of the curve and whose current spectrum Is (t) in Figure 18 shows a reduction in harmonics of less than 5%, that is to say THD = 3.59%.

TABLE 2: INTERPRETATION OF PERFORMANCE FOR THE TWO ORDERS

	PWM Control	**DCM Control**	**SLDCM Control**
THD before filtering	28,19%	28,19%	28,19%
THD after filtering	1.72%	0.79%	3.59%.
Main voltage	220V	220V	220V
Controllability of the switching frequency	good	good	Bad
Waveform of output current Is	good	Good	Fairly good

Table 2 gives an interpretation of the results obtained for Hysteresis and Cyclic Ratio Modulation (DCM) control. THD of the current at phase (a) Is(t) after filtering calculated on the first 20 harmonic ranks is 1.72% for PWM control. 0.79% for DCM control, and 3.59% for SLDCM which corresponds to the IEEE 519 standard that limits the THD < 5%, but it can be seen that control by DCM has better performance in terms of harmonic elimination, it is easy to use, ensures operation at a fixed frequency.

CONCLUSION

In this article, we have presented the method of instantaneous powers for the creation of disturbance currents; a mathematical model has been developed. We used PWM control DCM and SLDCM commands for switching IGBTs. Their principle is based on the modulation of a reference voltage. This voltage, called the modulating signal at the input of the modulator, will be transposed into a modulated signal in the form of square waves representing the control signals of the IGBTs. These two systems were implemented and observed under the same conditions in an active shunt filter. Regarding the THD rate in the electrical circuit, the DCM gives the best performance because it is 0.79% against 1.72% for the PWM and 3.59% for SLDCM. but it can be seen that the DCM control has better performance in terms of harmonic elimination and is positioned in the literature as a promising method due to its flexibility and ease of implementation in industrial applications.
It will also be interesting to carry out an in-depth study between the intelligent controls techniques neural networks with DCM applied to control the inverter in an active shunt filter.

TABLE 3: COMPARISON OF METHODS IN THE LITERATURE

	PWM Intersective Control [21]	Hysteresis Control [16]	DCM Control
Waveform of output current	good	Fairly good	good
TDH before filtering	20,17%	26,57%	28,19
TDH after filtering	2.33%	3,12%	0.79%
Signal quality	No noise	Brute	No noise
Controllability of the switching frequency	Yes	No	Yes

The performance of the proposed active shunt filter control strategy was compared with the control strategy adopted with some other control methods proposed in the literature. Table 3 shows the comparison of various control techniques proposed in the literature for harmonic reduction. It is clearly established that all these methods give a THD < 5% thus complying with the IEEE-519 standard, but the control strategy using DCM with the shunt active filter topology proposed in this work is more flexible due to its simplicity of implementation and allows good controllability of the switching frequency of the inverter switches that make up the active filter.

NOMENCLATURE

PWM	Pulse Wave Modulation
DCM	Duty Cycle Modulation
GLDCM	General linear Duty Cycle Modulation
LNIDCM	Linearized Non-Inverter Duty Cycle Modulation
NIDCM	Non-Inverter Duty Cycle Modulation
THD	Total Harmonic Distorsion
V_{ref}	Reference or control voltage
V_{sat}	Saturation voltage
$V_{sa,Vsb,Vsc}$	Output voltage
V_o	Integrator output voltage
Vc	Capacitor voltage

REFERENCES

[1] J. W. Dixon, J. J. Garcia, et L. Moran, « Control system for three-phase active power filter which simultaneously compensates power factor and unbalanced loads », *IEEE transactions on Industrial Electronics*, vol. 42, nº 6, p. 636-641, 1995.

[2] A. Sahbani, M. L.-B. Braiek, M. A. Dami, et M. Jemli, « Commande d'un filtre actif triphasé shunt par logique floue », 2005.

[3] H. Chaoui et P. Sicard, « Adaptive fuzzy logic control of permanent magnet synchronous machines with nonlinear friction », *IEEE Transactions on Industrial Electronics*, vol. 59, nº 2, p. 1123-1133, 2011.

[4] T. Yorozu, M. Hirano, K. Oka, et Y. Tagawa, « Electron spectroscopy studies on magneto-optical media and plastic substrate interface », *IEEE translation journal on magnetics in Japan*, vol. 2, nº 8, p. 740-741, 1987.

[5] A. F. H. Nohra, M. Fadel, et H. Y. Kanaan, « A novel instantaneous power based control method for a four-wire SAPF operating with highly perturbed mains voltages », in *2016 IEEE International Conference on Industrial Technology (ICIT)*, 2016, p. 1236-1241.

[6] M. Moranchel, F. Huerta, I. Sanz, E. Bueno, et F. J. Rodríguez, « A comparison of modulation techniques for modular multilevel converters », *Energies*, vol. 9, nº 12, p. 1091, 2016.

[7] S. K. Peddapelli, *Pulse Width Modulation*. De Gruyter Oldenbourg, 2016.

[8] L. N. Nnem, B. M. Lonla, G. B. Sonfack, et J. Mbihi, « Review of a multipurpose duty-cycle modulation technology in electrical and electronics engineering », *Journal of Electrical Engineering, Electronics, Control and Computer Science*, vol. 4, nº 2, p. 9-18, 2018.

[9] J. Mbihi, B. Ndjali, et M. Mbouenda, « Modelling and simulation of a class of duty-cycle modulators for industrial instrumentation », 2005.

[10] J. Mbihi, F. Beng, martin kom, et L. Nneme, « A Novel Analog-to-digital conversion Technique using nonlinear duty-cycle modulation », *International Journal of Electronics and Computer Science Engineering*, vol. 7, janv. 2013.

[11] J. Mbihi et L. N. Nneme, « A multi-channel analog-to-Digital conversion technique using parallel duty-cycle modulation », *International Journal of Electronics and Computer Science Engineering*, vol. 1, nº 3, p. 826-833, 2012.

[12] J. Mbihi et L. N. Nneme, « A novel control scheme for buck power converters using duty-cycle modulation », *International Journal of power electronics*, vol. 5, nº 3-4, p. 185-199, 2013.

[13] B. L. Moffo, J. Mbihi, et L. N. Nneme, « A low cost and high quality duty-cycle modulation scheme and applications », *International Journal of Electrical, Computer, Energetic, Electronic and communication Engineering*, vol. 8, nº 3, p. 82-88, 2014.

[14] L. N. Nneme et J. Mbihi, « Modeling and simulation of a new duty-cycle modulation scheme for signal transmission systems », *American Journal of Electrical and Electronic Engineering*, vol. 2, nº 3, p. 82-87, 2014.

[15] J. Mbihi, « Dynamic modelling and virtual simulation of digital duty-cycle modulation control drivers », *International Journal of Electrical, Computer, Energetic, Electronic and Communication Engineering*, vol. 11, nº 4, p. 472-477, 2017.

[16] P. NNa et E. Ndjakomo, « Harmonic Pollution Control of the Electrical Network by Three-Phase Shunt Active Filter: Comparative Study of Controls, by Hysteresis and by Duty Cycle Modulation », *World Academy of Science, Engineering and Technology International Journal of Energy and Power Engineering*, 2020.

[17] G. Ngaleu, C. Kom, T. Yeremou, S. Eke, et A. Nanfak, « Design of New Duty-Cycle Modulator Structures for Industrials Applications, an Alternative to Pulse-Width Modulation », *European Journal of Electrical Engineering*, vol. 23, p. 103-111, juin 2021, doi: 10.18280/ejee.230203.

[18] A. T. Boum, G. B. Djidjio Keubeng, et L. Bitjoka, « Sliding mode control of a three-phase parallel active filter based on a two-level voltage converter », *Systems Science & Control Engineering*, vol. 5, nº 1, p. 535-543, 2017.

[19] L. Benchaita et S. Saadate, « A comparison of voltage source and current source shunt active filter by simulation and experimentation », *IEEE transactions on power systems*, vol. 14, nº 2, p. 642-647, 1999.

[20] L. F. Rafanotsimiva, G. Besançon, D. Georges, E. J. R. Sambatra, et J. M. Razafimahenina, « Modélisation multimodèle et commande par Compensation Parallèle Distribuée d'un système SMIB », *MADA-ENELSA*, vol. 1, p. 18-26, 2013.

[21] A. Morsli et A. Tlemçani, « Dépollution des Réseaux Electriques Basse Tension utilisant un Filtre Actif Parallèle à deux niveaux contrôlé par l'Algorithme P-Q », vol. 53, nº 2, p. 7, 2012.